Fundamentals of designing Cylindrical High Order Transformation Optics Invisibility Cloaks using Silver-Silica Metamaterials

Kareem S. Elassy[1*], Nadia H. Rafat[2,3], Mohamed E. Khedr[1], Moustafa H. Aly[1,3]
[1]Arab Academy for Science Technology and Maritime Transport, Electronics and Communications Department
[2] Cairo University, Faculty of Engineering, Engineering Mathematics and Physics Department
[3]OSA Member
*kareemsalah@ieee.org

Abstract

Metamaterials have effective properties that are distinctive from their composites as they consist of engineered designed properties that are not in nature. In order to be able to design a metamaterial, we should establish sufficient understanding of the properties of the constituents. This will enable us to engineer new effective parameters of the metamaterial. We shall perform a detailed analytical study for the effective parameters and the constituents' parameters of silver-silica metamaterial. This will define the optical response of the mixture at different sizes of the inclusions' and different volume fractions of the silver and silica. Also an optimum value of the volume fraction value is proposed to achieve a broadened resonance optical response. Finally, we propose the design technique and constraints of a non-magnetic optical cloaking device, based on high order transformation optics with different volume fractions of silver and silica.

Keywords—(Silver-Silica mixture, Effective Parameters, Transformation Optics, Invisibility cloak)

1. Introduction

The use of Metamaterials applications is expanding widely by the day. They are applied in negative index materials [1] super lens [2], hyper lens [3], black holes [4], chiral Metamaterials [5] as well as a variety of invisibility cloaks such as carpet cloaks [6], non-magnetic cloaks [7], magnetic cloaks [8] and other transformation optics cloaks [9]. The unique characteristic of metamaterial that it is designed to be compatible with tailored-desired properties that are based on the shape and volume fraction of a structural unit called meat-atoms. A key feature of manipulating the metamaterials' optical response is the presence of nano-metals in the structural unit, and what is vital about the metals, especially at the nano scale, is the surface plasmons that act as the gate for the propagation of the electromagnetic wave inside the metamaterials [10].

Our study is based on Bruggeman effective medium theory (EMT) [11]. We start with analyzing the silica dielectric parameters followed by the optical response of the metals and then the composite structure response. We then introduce the theory of invisibility cloaking using metamaterials, as we shall propose a design technique of the parameters considering the constraints for a particular geometric shape of non-magnetic cloak proposed by Shalaev in [12].

2. Theory of Metal-dielectric Composites

2.1. The Optical Response of a Typical Dielectric (Silica)

The permittivity of a typical dielectric is not a real positive for all the optical range. Figure 1 shows the frequency-dependent permittivity of a typical dielectric such as Silica.

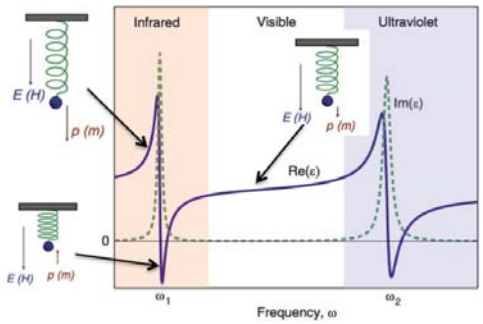

Figure 1: ε(ω) of a typical dielectric with 2 resonant frequencies [13].

Figure 1 shows two resonant frequencies ω_1 and ω_2. ω_1 occurs in the mid-infrared range due to photon absorption of the core electrons. ω_2 occurs in the ultraviolet range due to the band gap of the crystal [13]. The peaks in Figure 1 indicate material losses, and in-between the two resonances; $\varepsilon'(\omega)$ is approximately constant positive real. However, the optical response of Fused Silica at the nano scale is different from the bulk response [14]. Slightly after each resonance, the real part of $\varepsilon(\omega)$ for dielectrics can take negative values, thus the response of the material in this range is opposite to the driving force of the applied field [13].

2.2. The Optical Response of a Metal (Silver)

The real part of the dielectric function for noble metals is distinctively negative. The oscillation of free electrons is out of phase with respect to the driving field. Therefore, at the interface between a metal and a dielectric, most of the incident photons are reflected back [13].

$$\varepsilon(\omega) = \varepsilon'(\omega) + i\varepsilon''(\omega) = \varepsilon_\infty - \frac{\omega_p^2}{\omega^2} + i\frac{\omega_p^2\Gamma_1}{\omega^3} \quad (1)$$

$$\Gamma_1 = \Gamma + \frac{v_F}{R} \quad (2)$$

$\varepsilon(\omega)$ shows almost same response at different values of ε_∞, which accounts for the interband transitions [15] , and v_F indicates the material's Fermi velocity [13].
At optical frequencies, the effect of the modified damping constant Γ_1 will be dominant for $\varepsilon''(\omega)$ in (1). Therefore $\varepsilon''(\omega)$ will depend on the metal size particle R in (2).

The width of the surface plasmon resonance of metallic particles increases as the particle size decreases due to confinement effects that modify the metal dielectric function. This effect is developed from the change in the mean free path of the electrons, as the physical boundary of the metal particles becomes less than the physical mean free path. Given that Γ_1 depends on the mean free path therefore $\varepsilon''(\omega)$ will be affected. In the limit of very low particle concentration, particle size can be directly related to the plasmon width [16-17]. More details about the optical properties of silver at nano scale are in [18]. Figure 2 shows $\varepsilon'(\omega)$ and $\varepsilon''(\omega)$ versus the wavelength for bulk silver, while Figure 3 show $\varepsilon''(\omega)$ at different sizes of silver particles. It is noticeable that when the dimension of the metal is tens of nanometers, $\varepsilon''(\omega)$ is larger than its bulk value. This feature should be considered in the design of optical metamaterials with metal-dielectric meta-atoms [19].

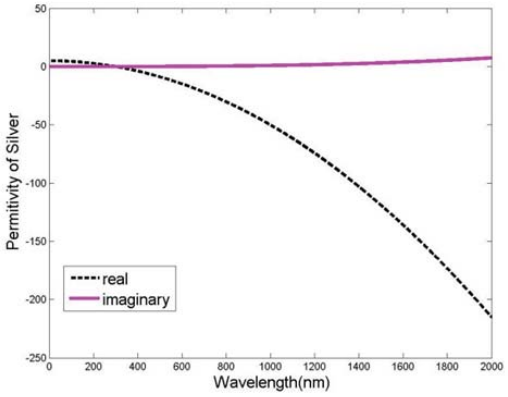

Figure 2: $\varepsilon'(\omega)$ and $\varepsilon''(\omega)$ of bulk silver.

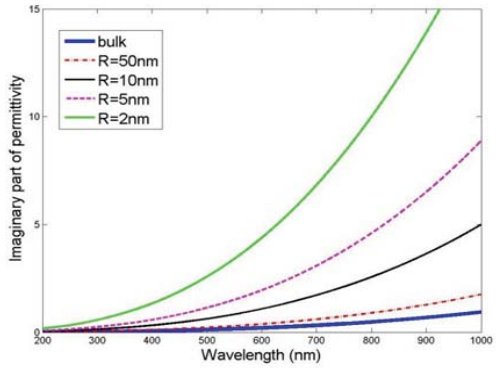

Figure 3: $\varepsilon''(\omega)$ of silver spherical particles at different sizes

This point can be illustrated through studying the refractive index of metal. From (1), we can obtain the complex refractive index of metals. At optical frequencies, $\varepsilon'' < |\varepsilon'|$ holds the permittivity function of metals. Therefore, the refractive index has a pronounced imaginary part while the real part of the index is only slightly larger than zero [13]. From the Fresnel equations, we understand that the coefficient reflection expressed by $(n_1 - n_2)/(n_1 + n_2)$ must have an absolute value of unity [20] when n_1 is real and n_2 is purely imaginary. As a result, at the boundary between a dielectric and a noble metal, almost all light is reflected as long as the wavelength is substantially longer than that of the interband transitions. Another phenomenon resulting from the large value of n'' is that light can only penetrate through a very thin layer of the noble metals. This travelling distance called the skin depth is the inverse of the absorption [15].

2.3. The Optical Response of a Silver-Silica Composite

In order to estimate the effective parameters of a composite medium without being restricted by the low filling factor cases for the Maxwell–Garnett theory (MGT), Bruggeman managed the two constituent materials on equal footing. The technique is based on assuming two complementary inclusions in a host, where $f_1 + f_2 = 1$ [21], and that the host is the effective parameter. The expression for the effective permittivity of the composite is stated in (3).

$$\varepsilon_{eff} = \frac{1}{4}\{(3f_1 - 1)\varepsilon_1 + (3f_2 - 1)\varepsilon_2 \pm\sqrt{[(3f_1 - 1)\varepsilon_1 + (3f_2 - 1)\varepsilon_2]^2 + 8\varepsilon_1\,\varepsilon_2}\ \} \quad (3)$$

where ε_{eff} is the effective permittivity, ε_1 is the permittivity of the metal inclusions, ε_2 is the permittivity of the dielectric which is equal to 3.8 for the silica at the visible range, f_1 and f_2 are the filling fraction of the metal and the dielectric in the composite respectively. Metal-dielectric composites with effective permittivity in (3) that comply can show a negative real part of the effective permittivity function ($\mathrm{Re}\{\varepsilon_{eff}\} < 0$), which its absolute value can be adjusted by controlling the filling fraction [21] as shown in Figure 4.a and 4.b. As concentration increases the interaction among particles induces additional broadening.

Bruggeman's Effective Medium Theory (EMT) predicts a critical filling fraction for metal, which is known as the percolation threshold. It represents the minimum volume fraction of conducting particles needed for the formation of a continuous conducting pathway [11]. In Figure 4.b, we see that the resonance band in ε_{eff} is very broad in the curve where f=0.4. In fact, this peak can extend to an infinite bandwidth if the filling fraction approaches 1/3, which is the percolation threshold for the silver-silica composite [13]. The percolation in a mixture indicates that the magnitude of the metal permittivity $|\varepsilon_1|$ is much larger than the permittivity of the dielectric component ε_2. The real part of ε_{eff} approaches the silver permittivity with increasing metal filling fraction f , which is a rather intuitive result. Interestingly, the imaginary part of ε_{eff} shows a broadened resonance peak due to the electromagnetic interactions between the metal and dielectric grains. If the constitutes of

this mixtures is arranged to form a planar arrays of nearly-touching metallic nanoparticles, thus yielding well confined guided mode [22].

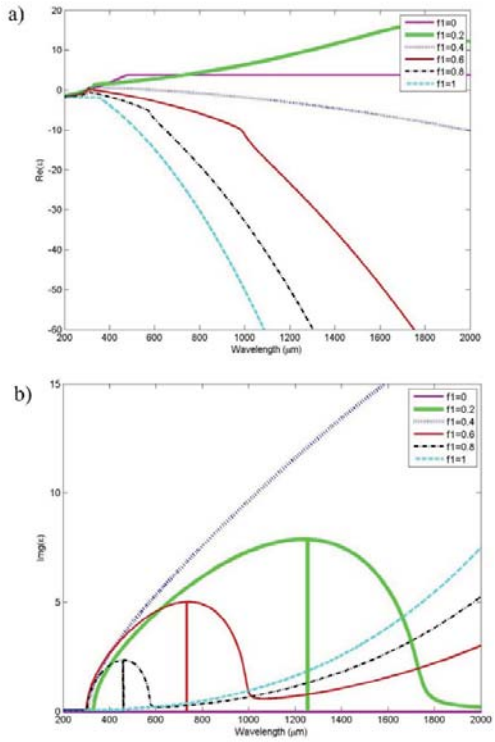

Figure 4: a) $\varepsilon'_{eff}(\omega)$ and b) $\varepsilon''_{eff}(\omega)$ of silver-silica composites at different metal volume fractions.

Figures 5-8 show the real and the imaginary part of the effective permittivity of silver-silica composites for different sizes of silver inclusion R at different volume fractions f from f=0.2 to f=0.8. The two extreme cases at f=0 and f=1 will result in the electric response of the pure dielectric and pure metal respectively. By increasing the value of the volume fraction the composite approaches a pure metal level, this explains the decrement of the value of the real part of the effective permittivity from 3.8 at f=0 till it reaches a negative value at volume f=1.

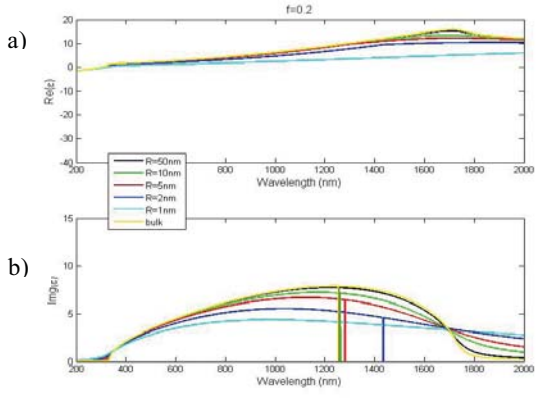

Figure 5: a) $\varepsilon'_{eff}(\omega)$ and b) $\varepsilon''_{eff}(\omega)$ for different sizes of silver inclusion at volume fraction (f=0.2).

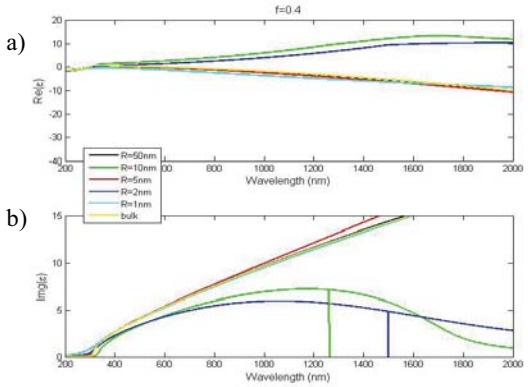

Figure 6: a) $\varepsilon'_{eff}(\omega)$ and b) $\varepsilon''_{eff}(\omega)$ for different sizes of silver inclusion at volume fraction (f=0.4).

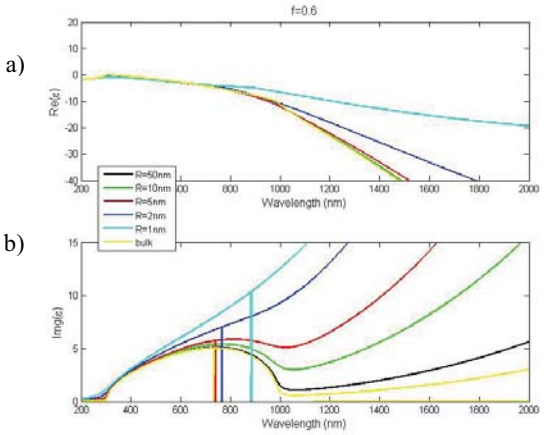

Figure 7: a) $\varepsilon'_{eff}(\omega)$ and b) $\varepsilon''_{eff}(\omega)$ for different sizes of silver inclusion at volume fraction (f=0.6).

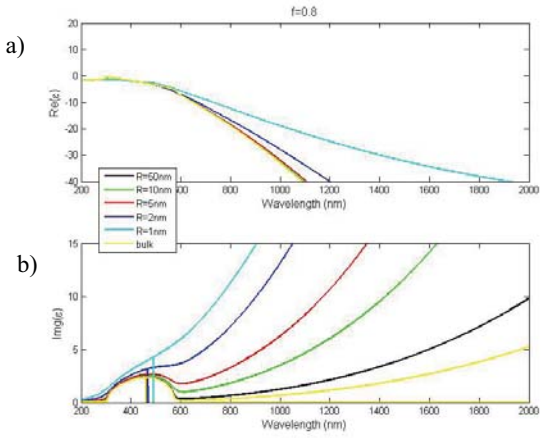

Figure 8: a) $\varepsilon'_{eff}(\omega)$ and b) $\varepsilon''_{eff}(\omega)$ for different sizes of silver inclusion at volume fraction (f=0.8).

The imaginary part of the effective permittivity shows a broadened resonance peak due to the electromagnetic interaction between the metals and the dielectric substrate. The metal-dielectric composite acts as a dielectric medium

for small metal concentrations of less than one third of the volume fraction, beyond the percolation threshold which occurs at f=0.4 as shown in Figure 6.b. The percolation threshold is the minimum volume fraction that satisfies the mixture will conduct (surface plasmons allow propagation of wave).

It is observed in Figures 5-8.b that the broadened resonance of $\mathrm{Img}(\varepsilon_{\mathrm{eff}})$ increases from f=0 (pure dielectric) to a maximum value of f=0.4, then decreases from f=0.6 until it reaches zero at f=1 (pure metal). It is noted that the highest sufficient coupling level is achieved between the electromagnetic wave and the metamaterials when f=0.4. This is also can be observed from
Figure.

3. Design of Non-magnetic Optical Cloaking Device

After studying the optical response of a metal-dielectric composite, a precise control over the effective permittivity is valid. By adjusting the volume fractions of the constituent materials, a graded permittivity profile can be achieved.

In this section, we propose a design technique for a non-magnetic optical cloaking device with a geometrical structure previously proposed in [23]. For non-magnetic cloaking; only the permittivity of the material is varied and modified while the permeability remains constant for the whole cloak μ=1. There are many theoretical approaches to achieve optical cloaking, such as Quasi-conformal mapping, Mei Scattering and Transformation optics (TO), TO will be used in this piece of work. Transformation optics is a field of a study that enables a precise control over electromagnetic fields by distorting the Cartesian coordinate system according to the design at will.

$$r = [1 - a/b]r' + a \tag{4}$$

$$r = [(a/b)(r'/b - 2) + 1]r' + a \tag{5}$$

For a cylindrical geometry as shown in 10, we perform a transformation function $\mathrm{r} = \mathrm{g}(\mathrm{r}')$ from $(\mathrm{r}', \theta', \mathrm{z}')$ to $(\mathrm{r}, \theta, \mathrm{z})$. This transformation compresses the region $\mathrm{r}' < \mathrm{b}$ to a concentric shell $\mathrm{a} < \mathrm{r} < \mathrm{b}$. The transformation function $\mathrm{r} = \mathrm{g}(\mathrm{r}')$ can be either a liner relation, expressed in (4), or a high order relation, as expressed in (5) [13].

$$\varepsilon_r = (r'/r)^2 \;;\; \varepsilon_\theta = [\partial \mathrm{g}(\mathrm{r}')/\partial r']^{-2} \;;\; \mu_z = 1 \tag{6}$$

From equation (5) and based on the techniques described in [24], the ε and μ tensors can be derived. We focus on TM incidence with the magnetic field polarized along the z axis. In this case only μ_z, ε_r and ε_θ enter into Maxwell's equations. The reduced set of non-magnetic TM-polarized cloak parameters is expressed in (6).

Equation (6) shows that ε_{r} varies from 0 at the inner boundary of the cloak (r = a) to 1 at the outer surface (r = b) [12]. The link between the mathematical equations and expressions derived from the transformation optics theory and the real-life application is Fermat principle. According to Fermat principle, the light travels in the direction that satisfies the maximum velocity. Given that Fermat principle is a function of the refractive index $n = \sqrt{\varepsilon\mu}$ and assuming non-magnetic cloak in which $\mu = 1$, therefore creating metamaterials with designed effective permittivity will provide the desired refractive index profile that control that path of light rays. This is achieved by setting controlled and continuous graded refractions.

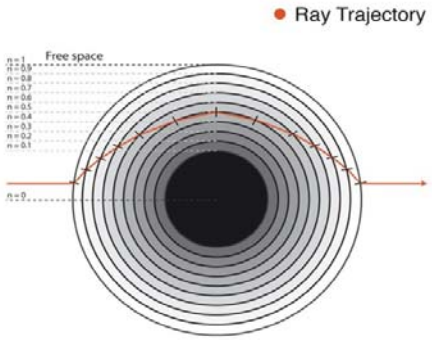

Figure 9: A light ray trajectory in a graded-index material

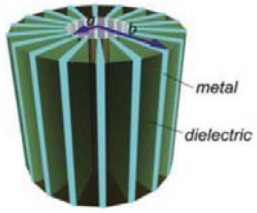

Figure 10: Schematic of a cylindrical non-magnetic cloak with high-order transformations for TM polarization [23].

Figure 10 shows a schematic of the design proposed in [23]. The device has a cylindrical geometry structure and is designed according to the high order transformation optics theory. We control the distortion of the coordinate system to achieve a ray trajectory as shown in Figure 9, the incident electromagnetic wave moves around the cloaked area $(r < a)$. This was achieved by creating a graded index material by controlling the tensors of permittivity that is expressed as ε_{r} and ε_θ in (7). The dielectric material that is used here is silica (silicon dioxide) and the metal is silver. We will subject the device to an electromagnetic wave of a wavelength of 532 nm. The electric permittivities of the two constituent materials at this wavelength are as follow: $\varepsilon_{\mathrm{SiO_2}} = 2.13$ and $\varepsilon_{\mathrm{Ag}} = -10.6 + 0.14\mathrm{i}$.

In order to manipulate the metamaterial effective parameters we must first analyze a periodically-layered composite with two isotropic constituent materials aligned in a parallel manner, as shown in Figure 11. The bulk permittivities of the two constituents are ε_1 and ε_2, respectively.

The volume filling fraction of material 1 is noted as f_1, so the second constituent has a filling factor $f_2 = 1 - f_1$.

In such a system, there are two principle situations to be studied: when the external electric field is either parallel or perpendicular to the planar interfaces.

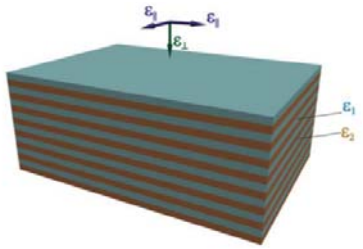

Figure 11: Schematic of a layered metal-dielectric structure, with the permittivities of the two constituents given as ε_1 and ε_2, respectively. Two principal effective permittivities, $\varepsilon_\parallel$ and $\varepsilon_\perp$ [13].

$$\varepsilon_\parallel = f_1\varepsilon_1 + f_2\varepsilon_2 \tag{7}$$

$$\varepsilon_\perp = \frac{\varepsilon_1\varepsilon_2}{f_2\varepsilon_1 + f_1\varepsilon_2} \tag{8}$$

The two extremes in equations (7) and (8) are called the Wiener bounds to permittivity, which indicate the absolute values of the effective permittivity of the whole composite in two extreme situations [13]. The Wiener bounds of a Silver-Silica layered composite are plotted in Figure 12.

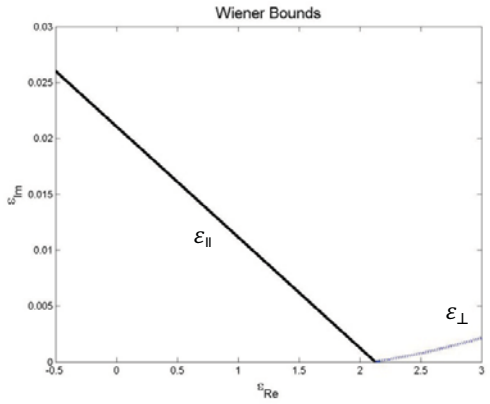

Figure 12: The Wiener bounds, $\varepsilon_\parallel$ and $\varepsilon_\perp$, of a Silver-Silica layered composite.

3.1. Constraints

Three main constraints must be put in consideration when designing the device. First, the main and most important constraint in the design is the thickness of the metal slabs, which shouldn't exceed the skin depth. As a result, the first step in designing the device is to calcite the skin depth of silver.

From (9), we can calculate the skin depth of the silver at the wavelength of the incident wave.

$$\delta = \frac{\lambda_0}{4\pi n''} \tag{9}$$

where δ is the skin depth, λ_0 is the wavelength of the wave and n'' is the imaginary part of the refractive index of silver.

Second, the device must satisfy a graded-index manner as the electromagnetic wave moves from the outer radius to the inner one. For a purely non-magnetic TM mode, equation (6) shows, as previously stated that ε_r varies from zero at the inner boundary of the cloak (r = a) to one at the outer surface (r = b) [13].

The third and final constraint is that the Silver-Silica building unit should not exceed, in size, the wavelength of the incident wave. This ensures that the light treats the whole composite as a new material with effective parameters rather than two separate materials with the constituents' parameters. The building unit for the design in Figure 10 is considered as the elementary arc that is repeated all over the cloak, thus the lattice parameter is the sum of the lengths of the metal and dielectric arcs - as shown in Figure 13. This length increases as gradually as we go away from the center, this should be considered because if this lattice parameter becomes greater than the incident wavelength the effective properties condition violates.

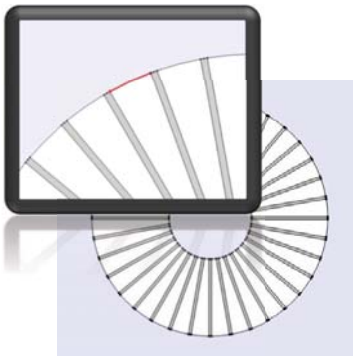

Figure 13: Top view of the cloak magnifying the elementary arc that is considered as the meta-atom.

3.2. Design Parameters

In this sub-section, we derive from the previous constraints the exact numerical values of the design parameters. Starting with the first constraint, which is the skin depth of Silver, and from equation (10), we find that the skin depth of Silver at wavelength $\lambda = 532\,nm$ is approximately equal to $13\,nm$. So we take the thickness of the Silver slap to be $10\,nm$.

In order to satisfy the second constraint -which is grading the refractive index from $n = 1$ at the outer boundary of the cloak to $n = 0$ at the inner boundary - we should derive the proper volume fractions of Silver and Silica at both boundaries. At the inner boundary, $(r = a)$, we derive the Silver volume fraction f_1 which satisfies the effective permittivity $\varepsilon_\parallel = 0$ from the Wiener bounds plotted in Figure 12. This is also expressed in equations (7) and (8).

First, we rearrange equation (7) in order to express f_1, the Silver volume fraction, in terms of $\varepsilon_{\parallel}, \varepsilon_1$, and ε_2, the effective permittivity, the Silver permittivity, and the Silica permittivity, respectively. We also note that $f_1 = 1 - f_2$. The final expression is stated in equation (10).

$$f_1 = \frac{\varepsilon_{\parallel} - \varepsilon_2}{\varepsilon_1 - \varepsilon_2} \tag{10}$$

For both boundaries, we substitute $\varepsilon_1(\varepsilon_{Ag}) = -10.6 + 0.14i$ and $\varepsilon_2(\varepsilon_{SiO_2}) = 2.13$. However, for the outer boundary of the cloak, we substitute $\varepsilon_{\parallel} = 1$, and for the inner boundary, we substitute $\varepsilon_{\parallel} = 0$. From these values, we conclude that $f_1|_{(r=b)} = 0.088767$ and $f_1|_{(r=a)} = 0.167321$.

$$f_1 = l_1/(l_1 + l_2) \quad ; \quad f_2 = l_2/(l_1 + l_2) \tag{11}$$

$$\frac{f_1}{f_2} = \frac{l_1}{l_2} \tag{12}$$

$$l_2 = l_1 \frac{f_2}{f_1} = l_1 \frac{1 - f_1}{f_1} \tag{13}$$

Since the thickness of the silver slap $l_1 = 10\ nm$ covers the entire cloak region ($a < r < b$), therefore we can calculate the lengths of the arcs at the outer and inner radii to satisfy the volume fractions, $f_1|_{(r=b)}$ and $f_1|_{(r=a)}$, which are derived from equation (10). We take the fundamental equations expressed in (11), where l_1 and l_2 are the lengths of the Silver and Silica, respectively, at any of the boundaries. From these expressions, we can derive a relation between the volume fractions of Silver and Silica in terms of their lengths, as shown in equation (12). Finally, equation (13) states the length of Silica l_2 in terms of f_1, f_2 and l_1.

As discussed before, and from the nature of the geometry of the design, we substitute $l_1 = 10\ nm$ for both boundaries of the cloak. At the outer boundary ($r = b$), we substitute with the proper volume fractions from equation (10) into equation (13), and the same is performed at the inner boundary ($r = a$). From these two conditions, we can derive the length of Silica arc at both boundaries $l_2|_{(r=b)} = 102.65\ nm$ and $l_2|_{(r=a)} = 49.77\ nm$.

Before we can determine the lengths of the inner and outer radii, a and b respectively, we should assume the angle between the Silver slabs. We take this angle $\phi = 3^0$ (in degree) and $\phi = \frac{1}{60}\pi$ (in radians).

$$a = \frac{l_1 + l_2|_{(r=a)}}{\phi|_{rad}} \tag{14}$$

$$b = \frac{l_1 + l_2|_{(r=b)}}{\phi|_{rad}} \tag{15}$$

After substituting directly in equations (14) and (15), we can derive $a = 1.14\ \mu m$ and $b = 2.15\ \mu m$.

Table 1: The parameters needed to design the optical cloaking device with the value for each parameter.

Parameter	Symbol	Value
Inner radius	a	$1.14\ \mu m$
Outer radius	b	$2.15\ \mu m$
Silver slap thickness	l_1	$10\ nm$
Angle between slaps	ϕ	3^0

Figure 14 shows the numerical simulation result of TM polarized EM wave incident from the right side, the wave is mapped around the cloaked region that is coated with silver layer at the inner cylinder. The simulation is carried out using FEM COMSOL Multiphysics commercial package.

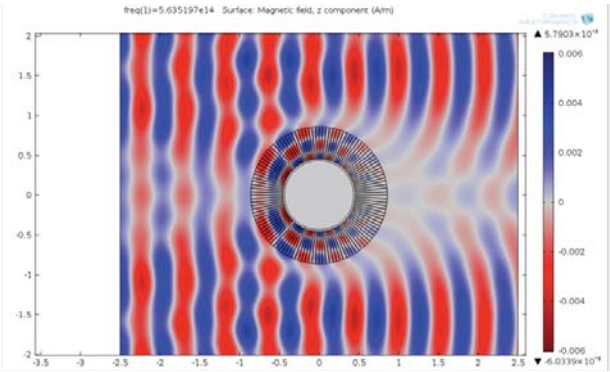

Figure 14: Simulation of the magnetic field mapping around the cloaked region with TM illumination at λ=532.8 nm.

4. Conclusion

From our study for the optical response of silver-silica composite metamaterial we have concluded that the parameters of the mixture responses in an independent manner from constituents of the metamaterial. It depends mainly on the structure of the meta-atom. We studied the parameters of the typical Silica, then the parameters of the silver particles at different sizes, then the effective parameters of silver-silica composite at different volume fractions and different sizes of the metal particles. We have shown that the optical response changes correspondingly according to the volume fraction of the component. Also, we have demonstrated the critical volume fraction for the silver in which the metamaterials broadened resonance response, due to the propagation of the surface plasmons oscillation.

After discussing the required properties to design a non-magnetic optical cloaking device, we analyzed the bulk permittivity of parallel-layered composites of isotropic constituents till we reached the two extremes of Wiener bounds. We used the cylindrical geometric shape of silica and metal slabs which was designed according to high order TO. It is evident that we faced three constraints, the main constraint was the skin depth of the metal slab which was

chosen to be 10nm, the second was the graded index manner that should varies 0 at the inner radius to 1 at the outer radius, and the last one was the length of the elementary arc which should be less λ of the incident light to sustain effective properties rather than independent responses of the constituents.

Acknowledgements

Many thanks to the members of the Real Engineer Program in the Arab Academy for Science Technology, and Maritime Transport for their help in this work.

References

[1] Park N, Min B A terahertz metamaterial with unnaturally high effective refractive index. Nature 470, 369-373, 2011.

[2] Scarborough C P Experimental demonstration of an isotropic metamaterial super lens with negative unity permeability at 8.5 MHz. Appl. Phys. Lett. 101, Issue: 1, 2012.

[3] Hakkarainen, Setälä T, Friberg AT Near-field imaging of interacting nano objects with metal and metamaterial superlenses. New J. Phys. 14 043019, 2012.

[4] Climente, Alfonso Omnidirectional broadband acoustic absorber based on metamaterials. Appl. Phys. Lett. 100, Issue: 14, 2012.

[5] Li Z, Alici KB, Caglayan H, Kafesaki M, Soukoulis CM, Ozbay E Composite chiral metamaterials with negative refractive index and high values of the figure of merit. Optics Express, Vol. 20, Issue 6, 6146-6156, 2012.

[6] Fischer J, Ergin T, Wegener M Three-dimensional polarization-independent visible-frequency carpet invisibility cloak. Opt. Lett. 36, 2059-2061, 2011

[7] Huang L, Zhou D, Wang J, Li Z, Chen X, Lu W Generalized transformation for nonmagnetic invisibility cloak with minimized scattering. JOSA B, Vol. 28, Issue 4, 922-928, 2011

[8] Gömöry F, Solovyov M, Šoucl J, Navau C, Prat-Camps J, Sanchez A Experimental realization of a magnetic cloak. Science, Vol. 335, No. 6075, 1466-1468, 2012.

[9] Chen H, Chan CT, Sheng P Transformation optics and metamaterials. Nature Materials 9, 387-396, 2010.

[10] Vladimir M. Shalaev (2006), "ECE 695s Nanophotonics Lecture 3," https://nanohub.org/resources/1748.

[11] Sancho-Parramon J, Janicki V, Zorc H On the dielectric function tuning of random metal-dielectric nanocomposites for metamaterial applications. Optics Express, Vol. 18, Issue 26, 26915-26928, 2010.

[12] Cai WS, Chettiar UK, Kildishev AV, Shalaev VM Optical cloaking with metamaterials. Nat. Photonics **1**, 224-227, 2007.

[13] Shalaev VM, Cai W. Optical metamaterials: fundamentals and applications. DOI 10.1007/978-1-4419-1151-3. Springer Science+Business, 2010.

[14] Miloslavsky VK, Makovetsky ED, Ageev LA, Beloshenko KS Fused silica as a composite nanostructured material. Optika Spektroskopiya, 2009, Vol. 107, No. 5, 854–859, 2009.

[15] Pinchuk A, von Plessen G, Kreibig U Influence of interband electronic transitions on the optical absorption in metallic nanoparticles. J. Phys. D: Appl. Phys. 37 3133, 2004.

[16] Sancho-Parramon J Surface plasmon resonance broadening of metallic particles in the quasi-static approximation: a numerical study of size confinement and interparticle interaction effects. Nanotechnology, 20(23), 23576, 2009.

[17] Sancho-Parramon J, Janicki V, Loncari M, Zorc H, Dubcek P, Bernstroff S, Optical and structural properties of Au-Ag islands films for plasmonic applications, 2011

[18] Kelly KL Coronado E, Zhao LL, Schatz GC J The Optical Properties of Metal Nanoparticles: The Influence of Size, Shape, and Dielectric Environment. Phys. Chem. B, 107 (3), 668-677, 2003.

[19] Sonnichsen C, Plasmons in metal nanostructures, A dissertation, University of Munich, 2001.

[20] Skaar J, Fresnel equations and the refractive index of active media, arXiv:physics/0509112v2 [physics.optics], 2006.

[21] Shalaev VM Nonlinear optics of random media: fractal composites and metal-dielectric film. (Springer Verlag, STMP-158, Berlin, Heidelberg,), 2000.

[22] Sainidou R, de Abajo G Plasmon guided modes in nanoparticle metamaterials. Opt. Express Vol. 16, Issue 7, pp. 4499-4506, 2008.

[23] Cai WS, Chettiar UK, Kildishev AV, Shalaev VM Designs for optical cloaking with high-order transformations. Opt Express 16:5444–5452, 2008.

[24] Pendry JB, Schurig D, Smith DR Controlling electromagnetic fields. Sci. Exp., 10.1126/science.1125907, 2006.